

## Article

# A New Model for Cleaning Small Cuttings in Extended-Reach Drilling Based on Dimensional Analysis

Liping Jin <sup>1,2</sup>, Gan Wang <sup>1,\*</sup>, Jingen Deng <sup>1</sup>, Ze Li <sup>3</sup>, Mingchi Zhu <sup>1</sup> and Rong Wang <sup>1</sup>

<sup>1</sup> MOE Key Laboratory of Petroleum Engineering, China University of Petroleum, Beijing 102249, China; jinlp@cnooc.com.cn (L.J.); dengjg@cup.edu.cn (J.D.); 2022215859@student.cup.edu.cn (M.Z.); 2022211016@student.cup.edu.cn (R.W.)

<sup>2</sup> CNOOC International Limited, Beijing 100010, China

<sup>3</sup> China Oilfield Services Limited, Langfang 065201, China; 2023310506@student.cup.edu.cn

\* Correspondence: wg\_sivan@163.com

**Abstract:** A wellbore's cleanliness affects drilling efficiency, economy and drilling safety directly in extended-reach drilling operations. Wellbore cleaning in extended-reach drilling has always been a tough problem. Field experience has shown that inefficient transport of small cuttings is a main factor for excessive drag and torque during extended-reach drilling. However, very little is known about the transport of small cuttings. In this paper, we use the data fitting method of dimensional analysis and regression analysis to establish a wellbore cleaning model for high-inclination sections, then use water and Polyanionic Cellulose (PAC) as a drilling fluid to analyze the settlement cleaning of small cuttings in the wellbore. The data from the example wells were used for field simulations to finally derive many factors like drilling fluid density, drilling fluid displacement, drill pipe rotation speed, diameter of cuttings and annulus hydraulic diameter, which affect the thickness of the dimensionless cutting bed. The results show that the dimensionless cutting thickness decreases with increasing drilling fluid density, drilling fluid displacement and drill pipe rotation speed; and increases with increasing cutting size and annular hydraulics diameter. Meanwhile, the effect of drilling fluid discharge, drill pipe rotation speed and cutting size on the thickness of the dimensionless cutting bed decreases as their values increase. This model can be utilized to design parameters in drilling and to predict the transport of cuttings in high-inclination sections. The successful establishment of the wellbore cleaning model for small cuttings in high-inclination sections of extended-reach drilling wells is highly innovative, which is a successful combination of theory and practice and has important guiding significance for promoting the development of wellbore cleaning technology.

**Keywords:** borehole cleaning; extended reach drilling; small cuttings



**Citation:** Jin, L.; Wang, G.; Deng, J.; Li, Z.; Zhu, M.; Wang, R. A New Model for Cleaning Small Cuttings in Extended-Reach Drilling Based on Dimensional Analysis. *Appl. Sci.* **2023**, *13*, 12118. <https://doi.org/10.3390/app132212118>

Academic Editor: Nikolaos Koukouras

Received: 18 September 2023

Revised: 23 October 2023

Accepted: 2 November 2023

Published: 7 November 2023



**Copyright:** © 2023 by the authors. Licensee MDPI, Basel, Switzerland. This article is an open access article distributed under the terms and conditions of the Creative Commons Attribution (CC BY) license (<https://creativecommons.org/licenses/by/4.0/>).

## 1. Introduction

In extended-reach drilling with high-inclination sections, small cuttings are easily influenced by gravity to gather at the bottom edge of the borehole and accumulate to form a cutting bed (Chen et al., 2018) [1]. Moreover, the gravity of small cuttings in a high-inclination section is smaller in the axial direction of the borehole than that of a straight or medium-inclination section and will not slide down the borehole in large quantities, thus forming a thick cutting bed. This leads to high levels of friction and a high resistance moment of the drill pipe, which causes serious drilling accidents (Guo et al., 2011) [2].

The transport of small cuttings in the drilling process of extended-reach drilling wells is a relatively complex physical process, and there are many factors affecting the movement and settlement of small cuttings. In order to understand the relevant laws affecting the transport of small cutting particles, scholars at home and abroad have conducted a lot of research on small-cutting cleaning models. These are mainly empirical models and stratification models based on mechanical analysis of theoretical models of small cutting cleaning in high-inclination well sections (Dang, 2017) [3]. Cho et al. (2002) [4] and Xing et al.

(2020) [5] studied the movement of annular small cutting particles in a three-layer cutting transport model, i.e., pure fluid layer, mixed suspension layer, and small cutting bed layer. Wang et al. (1993) [6], Wang et al. (2014) [7], Yuan et al. (2017) [8] and Chen et al. (2013) [9] investigated the various influencing factors on small cutting transport under different working conditions. Song et al. (2009) [10] and Sun et al. (2017) [11] analyzed the law influencing small cutting particle transport by analyzing the forces on small cuttings and considering the interaction forces generated between small cutting particles. At present, the cleaning models established by scholars produce large errors when calculating the transport process of small-sized cuttings, and there are only a few cleaning models specifically for small-sized cuttings. Therefore, in this paper, the cleaning model is derived and established by using the method of dimensional analysis and regression analysis for the cleaning of small-sized cuttings generated during the drilling process of extended-reach drilling wells.

**2. Model Building and Solution Methods**

*2.1. Force Analysis of Small Cuttings in a High-Inclination Well Section*

Figure 1 illustrates the various forces acting on small cuttings in extended-reach drilling and the direction of the forces. The forces acting on small-size cuttings include mainly net gravity, drag force, lift force, a tensile force due to uneven pressure distribution along the wellbore axis, and van der Waals force due to the interaction of adjacent small cuttings (Xiang et al., 2014) [12].

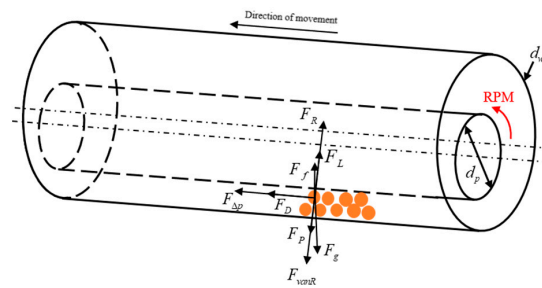


**Figure 1.** Diagram of forces on small-sized cuttings.

The expressions for the individual forces on the small cuttings are as follows.

The relative gravity of small-sized cutting particles in the annulus is the difference between gravity and buoyancy, which can be expressed as:

$$W = F_g - F_f = \frac{\pi d_c^2 (\rho_c - \rho_d) g}{6} \tag{1}$$

where the  $W$  is the relative gravity of small cuttings,  $F_g$  and  $F_f$  are the gravity and buoyancy of small cuttings,  $d_c$  is the diameter of the small cuttings,  $\rho_c$  and  $\rho_d$  are the density of the small cuttings and the density of the drilling fluid.

When small cutting particles move with the drilling fluid in the annular space, they are subjected to the same drag force as the axial direction of the borehole, which is expressed as:

$$F_D = \frac{1}{2} C_D A_p^* \rho_d v_{rp} |v_{rp}| \tag{2}$$

where  $F_D$  is the drag force on small cutting particles,  $C_D$  is the drag coefficient,  $A_p^*$  is the characteristic area and  $v_{rp}$  is the relative velocity of mud and small cuttings.

Due to the viscous effect of the drilling fluid, the velocities at different diameters at the same annular cross-section are different, and the velocity gradient around the small cuttings will produce a lifting force on it, which can be expressed as:

$$F_L = \frac{1}{2} \rho_d C_L v_{rp}^2 \left( \frac{\pi d_c^2}{4} \right) \tag{3}$$

where  $F_L$  is the lifting force of small cuttings and  $C_L$  is the lifting coefficient.

When drilling fluid flows axially along the borehole, an axial pressure gradient is generated, and the axial pressure gradient creates a pulling force along the borehole axis for small-sized cutting particles, which can be expressed as:

$$F_{\Delta P} = \frac{1}{6} \pi d_p^3 G_p \tag{4}$$

where  $G_p$  is the pressure gradient.

Due to the viscous effect of the drilling fluid, the drilling fluid will make a rotational motion with the rotation of the drill pipe, generating a tangential velocity perpendicular to the axial direction of the wellbore, making the drilling fluid velocity not be the same everywhere any longer, thus subjecting the small cuttings to the rotational lifting force of the drill pipe, expressed as:

$$F_R = \frac{\pi d_c^2}{8} C_{LR} \rho_d v_{PR} \tag{5}$$

where  $F_R$  is the rotational lift force of the drill pipe on small cuttings,  $C_{LR}$  is the rotational lift force coefficient of the drill pipe and  $v_{PR}$  is the flow velocity in the axial direction of the vertical borehole due to the rotation of the drill pipe.

The pressure caused by drilling fluid cementation is:

$$F_p = \frac{\pi}{4} d_c^2 \tau_y \tag{6}$$

where  $F_p$  is the pressure on small cuttings and  $\tau_y$  is the drilling fluid yield strength.

As the cuttings' diameter decreases and the surface area per unit volume increases, the Van der Waals force of molecular interactions between small cuttings has an impact on the cuttings' forces. The Van der Waals force between two small cuttings can be expressed as:

$$F_{van} = -\frac{A_H d_p}{24s^2} \tag{7}$$

where  $A_H$  is  $4.14 \times 10^{-20} \text{ N} \cdot \text{m}$ .  $s$  is the distance between two small cuttings.

Each small cutting is surrounded by an average of six small cuttings, and each one enclosed in the center interacts with each of the surrounding small cuttings in different directions, with the final combined force perpendicular to the surface of the cutting bed (Sun, 2014) [13]. The sizes are:

$$F_{vanR} = 6F_{van} \sin \phi \tag{8}$$

where  $\phi$  is the alignment angle of the cuttings, as shown in Figure 2.

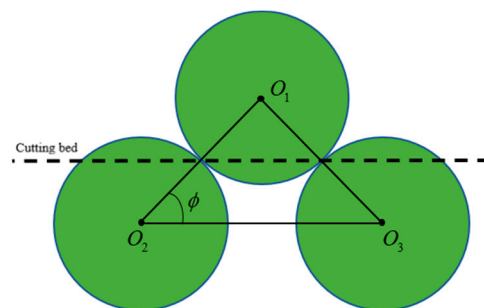


**Figure 2.** Arrangement angle diagram of small-sized cuttings.

### 2.2. Cleaning Model for a High-Inclination Well Section of the Wellbore

From the analysis in the previous section, it is clear that the van der Waals forces of particle interactions need to be considered for small cuttings relative to large cuttings. In addition, Duan et al. conducted extensive experiments on the motion of small cuttings

in the borehole annulus using an experimental setup similar to field scale (Duan et al., 2008) [14]. Ultimately, it was found that an error of up to 80% could be reached between the experimental results and the predicted values from the commonly used model built by performing a macroscopic forces analysis of the cutting bed. Therefore, it is necessary to develop a wellbore cleaning model that is easy to apply in the field for high-inclination sections of extended-reach drilling with small cutting particles.

The physical quantities involved in the wellbore cleaning problem in high-inclination sections of extended-reach drilling are wellbore size, well inclination angle, drill pipe eccentricity, drilling fluid flow rate, drilling fluid density, drilling fluid rheology, mechanical drilling speed, drill pipe speed, cutting size and cutting density (Sun et al., 2013) [15]. Using the method of dimensional analysis, each of these parameters is summarized and analyzed to derive a wellbore cleaning model, and then the model can be used more easily in the field with the help of regression analysis.

In this paper, it is assumed that the thickness of the cutting bed is uniform at rest, the cutting particles are spheres of equal diameter, the rheological properties of the drilling fluid are consistent with a steady-state incompressible non-Newtonian fluid, i.e., a power-law model drilling fluid, and the cutting particles do not affect the flow rate distribution of the drilling fluid.

The dimensionless cutting bed thickness was used as a discriminant to evaluate the drilling fluid’s efficiency in carrying small cuttings. The various parameters involved in the process are summarized, and the relationships between all parameters can be written as:

$$f\left(\frac{H, D_w, D_p, \theta, e, Q, v_d, \rho_d, \mu_e}{ROP, rpm, C_c, \rho_c, d_c, g, \Delta P, A_{bit}}\right) = 0 \tag{9}$$

Of which:

$$Q = \frac{\pi}{4} (D_w^2 - D_p^2) v_d \tag{10}$$

$$ROP = \frac{C_c R_t Q}{A_{bit}} \tag{11}$$

$$A_{bit} = \frac{\pi d_w^2}{4} \tag{12}$$

$$D_{hyd} = D_w - D_p \tag{13}$$

For power-law fluids:

$$\mu_e = K \left( \frac{2n + 1}{3n} \frac{D_w - D_p}{12v_d} \right)^{1-n} \tag{14}$$

where  $H$  is the thickness of the cutting bed,  $D_w$  is the diameter of the borehole and  $D_p$  is the outer diameter of the drill pipe.  $\theta$  is the well inclination angle,  $e$  is the drill pipe eccentricity,  $Q$  is the drilling fluid discharge,  $v_d$  is the drilling fluid upward return velocity,  $\mu_e$  is the apparent drilling fluid viscosity,  $ROP$  is the drilling speed,  $rpm$  is the drilling pipe speed,  $C_c$  is the small cutting volume concentration,  $\Delta P$  is the pressure difference,  $A_{bit}$  is the drill bit area,  $R_t$  is the quotient of cutting velocity and drilling fluid velocity,  $D_{hyd}$  is the annulus hydraulic diameter,  $n$  is the fluidity coefficient of the drilling fluid and  $K$  is the drilling fluid consistency coefficient.

Since drilling fluid discharge is a function of drilling fluid return rate and wellbore size; differential pressure is a function of wellbore size and shear stress, which in turn is a function of drilling fluid viscosity, drilling fluid return rate, and wellbore size; mechanical drilling speed is a function of small cutting volume concentration, bit area and drilling fluid discharge, which in turn is a function of borehole diameter; for power-law fluids,

drilling fluid viscosity is a function of the drilling fluid rheological parameters. Therefore, Equation (9) can be simplified to:

$$f(H, D_{hyd}, \theta, e, v_d, \rho_d, n, K, rpm, C_c, \rho_c, d_c, g) = 0 \tag{15}$$

There are 13 physical quantities involved during the transport of small cuttings, and the magnitudes and corresponding symbols of each variable are described in Table 1.

**Table 1.** The symbols and dimensions of the variables.

Symbols of Variables	Corresponding Scale
$D_{hyd}$	L
$\theta$	1
$e$	1
$v_d$	$LT^{-1}$
$\rho_d$	$ML^{-3}$
$n$	1
$K$	$ML^{-1}Tn^{-2}$
$rpm$	$T^{-1}$
$C_c$	1
$\rho_c$	$ML^{-3}$
$d_c$	L
$g$	$LT^{-2}$
$H$	L

In the wellbore cleaning problem of extended-reach drillings with high-inclination sections,  $D_{hyd}$ ,  $D_{hyd}$  and  $D_{hyd}$  are chosen as the basic physical quantities, and all other quantities can be obtained by these three basic quantities; the three basic measures chosen are the mass basic measure [M], the time basic measure [T], and the distance basic measure [L] (Sun, 2013) [16]. We can know that  $n = 13$  and  $m = 3$  according to the  $\Pi$  theorem, so there exist  $n - m = 10$  dimensionless physical quantities.

To solve for the dimensionless term  $\Pi_5$  of the drilling pipe speed, we have the following equation according to  $\Pi$  theorem:

$$\Pi_5 = D_{hyd}^a v_d^b \rho_d^c (rpm) \tag{16}$$

where  $a, b$  and  $c$  are factors to be determined.

Find the magnitudes of the variables from Table 1 and bring in:

$$\Pi_5 = (L)^a (LT^{-1})^b (ML^{-3})^c T^{-1} = L^{a+b-3c} T^{-b-1} M^c \tag{17}$$

By making the exponents of the three basic measures zero, we have:

$$\begin{cases} a + b - 3c = 0 \\ -b - 1 = 0 \\ c = 0 \end{cases} \tag{18}$$

The solution gives:  $a = 1, b = -1, c = 0$ .

The dimensionless term of drill pipe speed is:

$$\Pi_5 = D_{hyd} v_d^{-1} (rpm) = \frac{D_{hyd}(rpm)}{v_d} \tag{19}$$

The other dimensionless terms can be found in the same way and are expressed as follows:

$$\Pi_1 = \theta \tag{20}$$

$$\Pi_2 = e \tag{21}$$

$$\Pi_3 = n \tag{22}$$

$$\Pi_4 = \frac{K}{D_{hyd}^n \rho_d v_d^{2-n}} \tag{23}$$

$$\Pi_6 = C_{cs} \tag{24}$$

$$\Pi_7 = \frac{\rho_c}{\rho_d} \tag{25}$$

$$\Pi_8 = \frac{d_c}{D_{hyd}} \tag{26}$$

$$\Pi_9 = \frac{D_{hyd} g}{v_d^2} \tag{27}$$

$$\Pi_{10} = \frac{H}{D_{hyd}} \tag{28}$$

The relationship between each of the above dimensionless terms can be expressed as:

$$f(\Pi_1, \Pi_2, \Pi_3, \Pi_4, \Pi_5, \Pi_6, \Pi_7, \Pi_8, \Pi_9, \Pi_{10}) = 0 \tag{29}$$

Separate the cutting bed thickness dimensionless term:

$$\frac{H}{D_{hyd}} = \phi(\Pi_1, \Pi_2, \Pi_3, \Pi_4, \Pi_5, \Pi_6, \Pi_7, \Pi_8, \Pi_9) \tag{30}$$

The physical quantities are nonlinearly related to the thickness of the dimensionless cutting bed, so that Equation (24) can be expressed as:

$$\frac{H}{D_{hyd}} = a_0 [\Pi_1^{a_1} \Pi_2^{a_2} \Pi_3^{a_3} \Pi_4^{a_4} \Pi_5^{a_5} \Pi_6^{a_6} \Pi_7^{a_7} \Pi_8^{a_8} \Pi_9^{a_9}] \tag{31}$$

where  $a_0, a_1, a_2, a_3, a_4, a_5, a_6, a_7, a_8$  and  $a_9$  are factors to be determined.

Regression calculations were performed using the experimental data from the article by Duan et al. (2008) [14]. The data relevant to the calculation are shown in Table 2.

**Table 2.** The basic data used in the example well.

Symbols of Variables	Corresponding Scale
Parameters	Values
Drilling fluid density	1180 kg/m <sup>3</sup>
Drilling fluid flowability index	0.55
Drilling fluid consistency factor	0.64 kg·s <sup>n-2</sup> /m
Drill pipe speed	10.47 s <sup>-1</sup>
Displacement	0.03 m <sup>3</sup> /s
Drill pipe OD	0.127 m
Borehole diameter	0.2159 m
Cutting diameter	0.0003 m
Parameters	Values
Drilling fluid density	1180 kg/m <sup>3</sup>
Drilling fluid flowability index	0.55
Drilling fluid consistency factor	0.64 kg·s <sup>n-2</sup> /m

Since the experimental eccentricity of the drill pipe, the concentration of cutting injection, the density of cutting and the acceleration of gravity are constant values, as is the well inclination angle, the range of the well inclination angle obtained in the experiment has little impact on the thickness of the cutting bed, based on previous experience; thus, the dimensionless terms  $\Pi_1, \Pi_2, \Pi_6, \Pi_7$  and  $\Pi_9$  are not considered. Then, Equation (31) can be simplified as:

$$\frac{H}{D_{hyd}} = a_0 [\Pi_3^{a_3} \Pi_4^{a_4} \Pi_5^{a_5} \Pi_8^{a_8}] \tag{32}$$

When using water as the drilling fluid, using the least squares method yields fitting with the experimental data:

$$\frac{H}{D_{hyd}} = 1.2082 \left[ \begin{array}{c} n^{-0.1068} \left( \frac{k}{D_{hyd}^n \rho_d v_d^{2-n}} \right)^{0.0686} \\ \left( \frac{D_{hyd} rpm}{v_d} \right)^{-0.0034} \left( \frac{d_c}{D_{hyd}} \right)^{0.0059} \end{array} \right] \tag{33}$$

The thickness of the dimensionless cutting bed is expressed as:

$$\frac{H}{D_w} = 1.2082 \left[ \begin{array}{c} n^{-0.1068} \left( \frac{k}{D_{hyd}^n \rho_d v_d^{2-n}} \right)^{0.0686} \\ \left( \frac{D_{hyd} rpm}{v_d} \right)^{-0.0034} \left( \frac{d_c}{D_{hyd}} \right)^{0.0059} \end{array} \right] \frac{D_{hyd}}{D_w} \tag{34}$$

Figure 3 shows the comparison between the predicted values of the model and the experimental data when water is used as the drilling fluid. A total of 42 sets of data were used for data fitting. After the calculation and comparison, the mean square error for the three data fit lines was 7.438%, 5.247% and 6.731%, respectively, and it can be found that the error of most of the data is less than 8%, which meets the requirements of the model error at the drilling construction site.

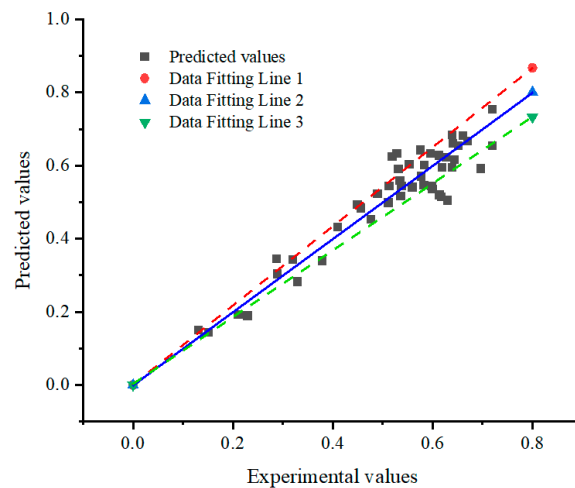


Figure 3. Comparing the experimental and predicted values of the dimensionless cuttings bed thickness.

When using Polyanionic Cellulose (PAC) as the drilling fluid, the same least-squares fit with the help of experimental data yields:

$$\frac{H}{D_{hyd}} = 3.4331 \left[ \begin{matrix} n^{-0.3553} \left( \frac{k}{D_{hyd}^n \rho_d v_d^{2-n}} \right)^{0.2228} \\ \left( \frac{D_{hyd} rpm}{v_d} \right)^{-0.0154} \left( \frac{d_c}{D_{hyd}} \right)^{0.0875} \end{matrix} \right] \quad (35)$$

The thickness of the dimensionless cutting bed is expressed as:

$$\frac{H}{D_w} = 3.4331 \left[ \begin{matrix} n^{-0.3553} \left( \frac{k}{D_{hyd}^n \rho_d v_d^{2-n}} \right)^{0.2228} \\ \left( \frac{D_{hyd} rpm}{v_d} \right)^{-0.0154} \left( \frac{d_c}{D_{hyd}} \right)^{0.0875} \end{matrix} \right] \frac{D_{hyd}}{D_w} \quad (36)$$

Figure 4 shows the comparison between the predicted values of the model and the experimental data when PAC is used as the drilling fluid; 52 sets of data were used for data fitting. After the calculation and comparison, the mean square error for the three data fit lines was 5.949%, 4.354% and 6.003%, respectively, and it can be found that the error of most of the data is less than 8%, which meets the requirements of the model error at the drilling construction site.

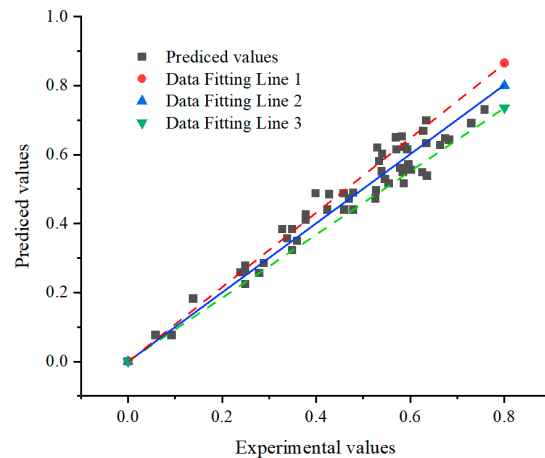


Figure 4. Comparing the experimental and predicted values of the dimensionless cutting bed thickness.

### 3. Case Application

An extended-reach drilling operation in the field with construction parameters closer to the conditions of Equation (36) was selected, and the model was used to perform an example calculation of the thickness of the dimensionless cutting bed in the high-inclination section of the extended-reach drilling wellbore, mainly analyzing the effects of factors such as drilling fluid density and drill pipe rotation speed (Chen et al., 2016) [17]. The relevant data of this example well required for the calculation are detailed in Table 2.

#### 3.1. Influence of Drilling Fluid Density on the Transport of Cutting Particles

During the drilling process, different types of drilling fluids also have a greater impact on the carrying and transport of cuttings. In order to investigate the effect of different drilling fluid densities on the movement pattern of cutting particles, the values of drilling fluid densities in a certain range are substituted into the resulting model, and other relevant parameters are kept constant. The variation law of the thickness of the

dimensionless cutting bed was obtained when the cutting diameter was 0.3 mm, 0.4 mm and 0.5 mm, respectively.

From Figure 5, it can be seen that the thickness of the dimensionless cutting bed is linearly and inversely related to the drilling fluid density at different cutting diameters. A higher drilling fluid density will produce a greater buoyancy force on small cuttings, which is conducive to the carrying of small cuttings by the drilling fluid, thus reducing the thickness of the dimensionless cutting bed.

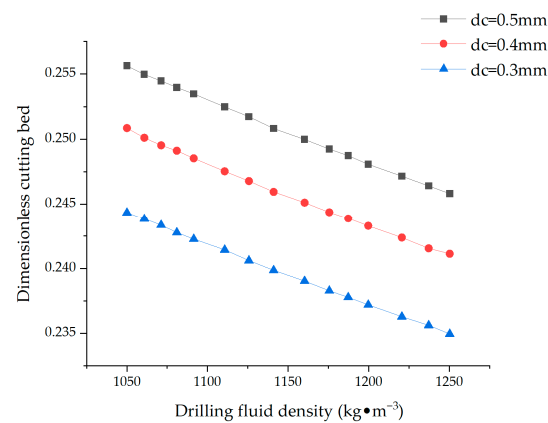


**Figure 5.** Effect of drilling fluid density on the thickness of dimensionless cuttings bed.

### 3.2. Influence of Displacement on the Transport of Cutting Particles

In the actual drilling process, the magnitude of the drilling fluid annular flow rate is regulated by the drilling fluid discharge, and the minimum value of the annular return velocity required to carry cutting particles for transport is determined according to the minimum drilling fluid discharge. When the annular flow rate is low, cuttings will accumulate on the lower side of the annulus and form a cutting bed (Jing et al., 2020) [18]. Therefore, the relationship between the drilling fluid discharge and the thickness of the dimensionless cutting bed needs to be further investigated. The drilling rod speed was set to 60 r/min, 110 r/min, and 160 r/min, and the joint model was used to study the effect of the drilling fluid discharge on the thickness of the dimensionless cutting bed.

Figure 6 shows that an increase in drilling fluid discharge results in a decrease in the thickness of the dimensionless cutting bed. The effect on the thickness of the dimensionless cutting bed slowly decreases with higher drilling fluid discharge. The effect of drilling fluid displacement is larger, and the drilling fluid displacement increases from 1100 L/min to 1400 L/min at a drill pipe rotation speed of 110 r/min, and the thickness of the dimensionless cutting bed decreases by 4.88%.

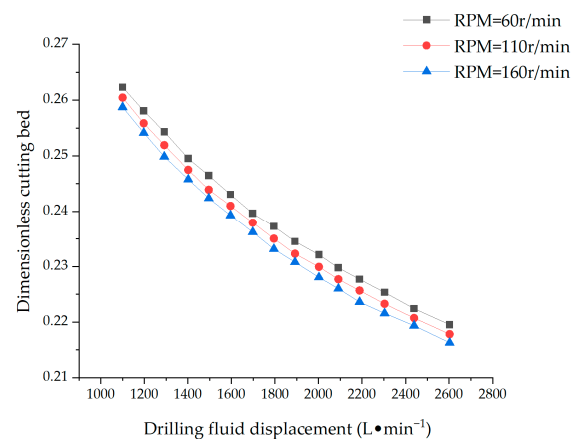


**Figure 6.** Effect of drilling fluid displacement on the thickness of dimensionless cuttings bed.

### 3.3. Influence of Drill Pipe Rotation Speed on the Transport of Cutting Particles

During the drilling of an extended-reach drilling operation, the rotation speed of the drill pipe also affects the cutting transport in the downhole annular flow path. The rotation of the drill pipe drives the drilling fluid to produce vortex flow, and the distribution of cutting particles producing a vortex state can be observed at the entrance. The mechanical scraping and churning action between the drill pipe and the cutting bed makes the drill pipe rotation disruptive to the cutting bed (Liu et al., 2019) [19]. In the study of the effect of drill stem rotation speed on the movement of cutting particles, the drill stem rotation speed was set between 60 r/min and 160 r/min, while the variation law of the thickness of the dimensionless cutting bed was calculated when the diameter of cutting particles was 0.3 mm, 0.4 mm, and 0.5 mm, respectively.

From Figure 7, it can be seen that the thickness of the dimensionless cutting bed is inversely related to the drill pipe rotation speed. The effect of increasing the drill pipe rotation speed decreases significantly at the same time. When the cutting diameter was 0.3 mm, the thickness of the dimensionless cutting bed decreased by 0.45% when the speed increased from 60 r/min to 80 r/min; when the speed increased from 140 r/min to 160 r/min, the thickness of the dimensionless cutting bed decreased by only 0.21%.

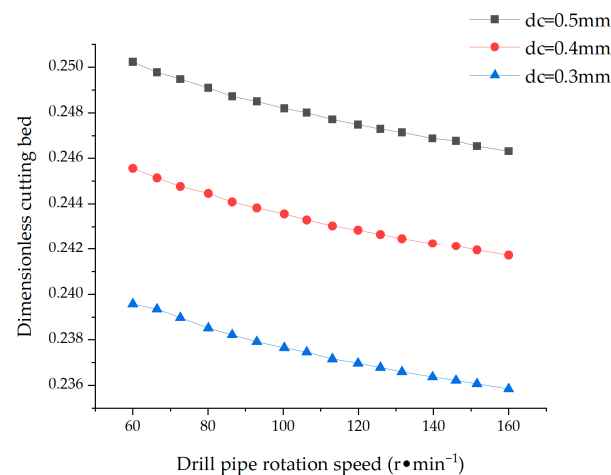


**Figure 7.** Effect of drill pipe rotation speed on the thickness of dimensionless cuttings bed.

### 3.4. Influence of Cutting Diameter on the Transport of Cutting Particles

For cuttings with the same density, small-sized particles can be stably suspended in the drilling fluid because their specific surface area is large and their own gravity does not exceed their viscous resistance: large-sized particles will rapidly settle to the well wall after generation, forming a stable bed of cuttings.

In the annular flow channel, the size of cutting particles also affects cutting transport: particles of a small size are easier to wash to the suspension layer, and the collision between particles does not affect cutting transport; particles of larger size are difficult to rise to the suspension layer due to gravity, and the collision between particles or between particles and the wall will affect the efficient transport of particles (Hu et al., 2022) [20].

Other conditions being unchanged, the influence of cutting diameter on the thickness of the dimensionless cutting bed was obtained by combining the model of settlement at a drilling fluid discharge of 1400 L/min, 1700 L/min, and 2000 L/min, respectively.

Under different cutting sizes, the increase in cutting diameter leads to the increase in the thickness of the dimensionless cutting bed, and the two show a quadratic curve relationship, as shown in Figure 8. The influence of cutting diameter on the thickness of the dimensionless cutting bed is larger when the diameter of small-size cuttings is less than 0.6 mm; once it is larger than 0.6 mm, the influence has a tendency to gradually decrease.

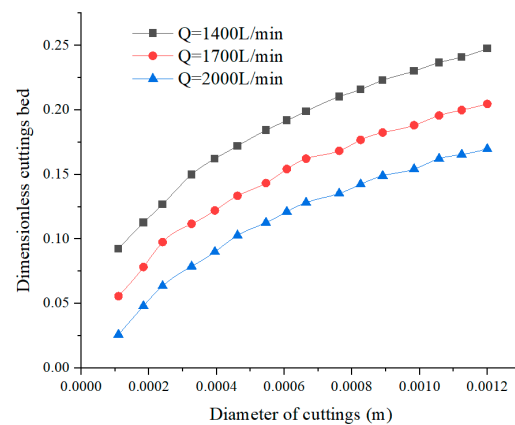


**Figure 8.** Effect of the diameter of cuttings on the thickness of the dimensionless cuttings bed.

### 3.5. Influence of Annulus Hydraulic Diameter on the Transport of Cutting Particles

In the drilling process, the size of the wellbore is also an important factor affecting the cleanliness of the cuttings. Different wellbore sizes represent different annular hydraulic diameters, however, the annular hydraulic diameter is one of the important factors affecting the drilling fluid return rate, so it is necessary to investigate cutting particle movement under different annular hydraulic diameters.

Using the basic data in Table 2, the wellbore dimensions of the example well were selected to calculate the thickness of the dimensionless cutting bed at different annular hydraulic diameters, and the wellbore dimensions were 311.15 mm × 139.7 mm, 215.9 mm × 127 mm and 152.4 mm × 88.9 mm.

From Figure 9, it can be seen that the thickness of the dimensionless cutting bed shows a positive relationship with the annulus hydraulic diameter. The analysis shows that the positive relationship exists mainly because a smaller annulus hydraulic diameter produces a larger drilling fluid return velocity under the condition of constant drilling fluid discharge, which is beneficial to the carrying of small-sized cuttings.

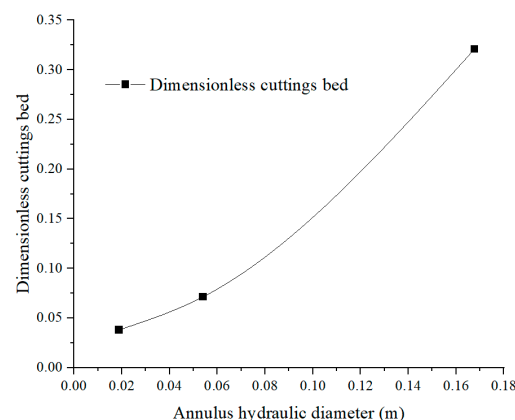


**Figure 9.** Effect of annulus hydraulic diameter on the thickness of dimensionless cuttings bed.

## 4. Conclusions

In this paper, a wellbore cleaning model is developed for extended-reach drilling with small cuttings in high-inclination sections based on the method of dimensional analysis and regression analysis. With the help of basic data from extended-reach drilling in the field, calculations are performed using the established model. The role of factors such as drilling fluid density and drill pipe rotation speed were investigated. The results show that the thickness of dimensionless cuttings bed decreases with increasing drilling fluid density, drilling fluid discharge, and drill pipe rotation speed, and increases with increasing cutting size and annular hydraulic diameter. Meanwhile, the effect of drilling fluid

discharge, drill pipe rotation speed, and cutting size on the thickness of dimensionless cutting bed decreases as their values increase. The successful establishment of the wellbore cleaning model for small-size cuttings in high-inclination sections of extended-reach drilling operations is highly innovative, which is a successful combination of theory and practice and has important guiding significance for promoting the development of wellbore cleaning technology.

**Author Contributions:** Conceptualization, G.W.; Methodology, L.J. and G.W.; Software, Z.L.; Validation, R.W.; Investigation, J.D.; Data curation, Z.L.; Writing—original draft, G.W.; Writing—review & editing, M.Z. All authors have read and agreed to the published version of the manuscript.

**Funding:** This research received no external funding.

**Institutional Review Board Statement:** Not applicable.

**Informed Consent Statement:** Not applicable.

**Data Availability Statement:** For the protection of research results, the data will not be disclosed.

**Acknowledgments:** This work was financially supported by a project of the Ministry of Industry and Information Technology of China (grant number: CBG2N21-4-2).

**Conflicts of Interest:** Author Liping Jin was employed by the company CNOOC International Limited. Author Ze Li was employed by the company China Oilfield Services Limited. The remaining authors declare that the research was conducted in the absence of any commercial or financial relationships that could be construed as a potential conflict of interest.

## References

1. Chen, X.Y.; Gao, D.L. The Maximum Allowable Well Depth While Drilling of Ultra-Extended-Reach Drilling from Shallow Water to Deepwater Target. *SPE J.* **2018**, *23*, 22–236. [[CrossRef](#)]
2. Guo, X.L.; Long, Z.H.; Wang, Z.M. Study of a simple method for calculating dynamic transport of cuttings in extended-r each drillings. *J. Oil Gas Technol.* **2011**, *33*, 108–111.
3. Dang, Y. *Optimization of Borehole Cleaning Technology for Offshore Extend-Reach Drilling*; Xi'an Shiyou University: Xi'an, China, 2017.
4. Cho, H.; Shah, S.N.; Osisanya, S.O.A. A three-segment hydraulic model for cuttings transport in coiled tubing horizontal and deviated drilling. *J. Can. Pet. Technol.* **2002**, *41*, 32–39. [[CrossRef](#)]
5. Xing, X.; Wu, Y.J.; Zhang, C. Hydraulic parameter optimization for drilling ultra-deep horizontal wells. *Fault-Block Oil Gas Field* **2020**, *27*, 381–385.
6. Wang, H.G.; Liu, X.S. Establishment of thickness model of cutting bed in horizontal well section. *J. China Univ. Pet. Ed. Nat. Sci.* **1993**, *17*, 8.
7. Wang, J.T.; Sun, B.J.; Li, H.; Xiang, H.F.; Wang, Z.Y.; Tian, A.M. Simulation analysis of cutting velocity distribution for drilling extended-reach horizontal wells. *Chin. J. Hydrodyn. Ser. A* **2014**, *6*, 739–748.
8. Yuan, L.F.; He, S.M.; Li, X.N.; Tang, M.; Shao, Y. Simulation study of annular flow considering drilling tool buckling. *Fault-Block Oil Gas Field* **2017**, *24*, 5.
9. Chen, X.P.; Wang, M.B.; Zhong, G.Y. Mechanical model for critical resuspension velocity of small cuttings in high-inclination well sections. *Fault-Block Oil Gas Field* **2013**, *20*, 4.
10. Song, X.C.; Guan, Z.C.; Chen, S.W. Mechanical model of critical annular flow velocity for cutting transport in inclined shafts. *J. China Univ. Pet. Ed. Nat. Sci.* **2009**, *33*, 5.
11. Sun, B.J.; Xiang, H.F.; Li, H. Model of the critical deposition velocity of cuttings in an inclined-slim hole annulus. *SPE J.* **2017**, *22*, 1213–1224. [[CrossRef](#)]
12. Xiang, H.F.; Sun, B.J.; Li, H.; Niu, H.B. Experimental study of cutting transport in extended-reach horizontal well section. *Oil Drill. Prod. Technol.* **2014**, *36*, 1–6.
13. Sun, X.F. *Experimental Study of Cutting Transport in High-Inclination Well Section and Optimal Design of Cleaning Tools*; Northeast Petroleum University: Daqing, China, 2014.
14. Duan, M.Q.; Miska, S.; Yu, M. Transport of small cuttings in extended-reach drilling. *SPE Drill AMP* **2008**, *23*, 258–265. [[CrossRef](#)]
15. Sun, X.F.; Yan, T.; Wang, K.L. Advances in borehole cleaning technology for complex structural wells. *Fault-Block Oil Gas Field* **2013**, *20*, 1–5.
16. Sun, B.H. Dimensional analysis and applications. *Phys. Eng.* **2016**, *26*, 11–20.
17. Chen, X.Y.; Gao, D.L.; Guo, B.Y.; Feng, Y.C. Real-time optimization of drilling parameters based on mechanical specific energy for rotating drilling with positive displacement motor in the hard formation. *J. Nat. Gas Sci. Eng.* **2016**, *35*, 686–694. [[CrossRef](#)]
18. Jing, S.; Xiao, S.; Zhang, H.L. Method for minimizing annular pressure consumption based on coupling borehole cleanliness and hydraulics. *Pet. Drill. Tech.* **2020**, *48*, 56–62.

19. Liu, C.W.; Li, Z.M. Advances in cutting transport modeling during drilling. *Drill. Fluid Complet. Fluid* **2019**, *36*, 663–671.
20. Hu, J.S.; Zhang, G.W.; Li, J.L. Numerical simulation analysis of cutting transport based on coupled CFD-DEM model. *Fault-Block Oil Gas Field* **2022**, *29*, 561–566.

**Disclaimer/Publisher's Note:** The statements, opinions and data contained in all publications are solely those of the individual author(s) and contributor(s) and not of MDPI and/or the editor(s). MDPI and/or the editor(s) disclaim responsibility for any injury to people or property resulting from any ideas, methods, instructions or products referred to in the content.